



**CHINA SHIP SCIENTIFIC RESEARCH CENTER**

**Sound Generation From a  
Moving Shell**

**Zhu Xiqing**

**June 1986**

**CSSRC Report  
English version 86005**

**P . O . BOX 116, WUXI, JIANGSU**

**CHINA**

# SOUND GENERATION FROM A MOVING SHELL

ZHU XIQING

China Ship Scientific Research Center

Wuxi, Jiangsu, China

## ABSTRACT

Noise generation by a moving shell with small ratio of length to width at high Reynolds number in water were studied. The interaction between the moving shell and surrounding fluid results in pressure fluctuations over the shell surface. The frequency spectra of the fluctuating pressure are different over the front part, the middle part and the rear of the shell.

The main sources of noise of the moving shell are velocity fluctuations generated by turbulent boundary layers and flow separations. The noise intensity outside the shell results from the reaction of the rigid shell to the fluctuating velocity and the shell vibration excited by it.

The cross - power spectral density of the noise inside the shell is proportional to the moving speed and the resistance coefficient.

The results of model experiment show that the power spectral density of the noise inside the two shells have differences of the order of 5 db. In order to reduce interior noise, the shell should have a proper shape.

## LIST OF SYMBOLS

$T_f, T_r$	frictional and form resistance on a unit area, respectively
$C_f, C_r$	frictional and form resistance coefficient, respectively
$U_o$	onset flow speed
$U_r, U_f$	fluctuating velocity
$\rho$	water density
$F_i$	fluctuating pressure
$p(\vec{x}, t)$	sound pressure
$r$	distance between origin and observation point
$\vec{x}$	distance between source and observation point
$U_n$	normal vibration velocity of shell
$s$	surface area of shell
$c$	sound velocity in water
$A_c, A_n$	correlation area
$t$	time
$\tau$	time interval
$\langle \{p(\vec{x}, t)\}^2 \rangle$	mean - square pressure
$I$	sound intensity
$W(n, \zeta, t)$	displacement of shell
$H_{mn}(\omega)$	function of frequency response
$Re$	Reynolds number
$M$	Mach number
$\xi, \eta, \zeta$	generalized coordinates
$R_n(r_{mn}\xi), \phi_n(\eta)$	eigenfunctions
$H_m(\zeta)$	
$m, n, p, q$	integer
$C_D$	total resistance coefficient

$\omega_{mn}$	eigenfrequency of shell
$K_z = \omega/U_0$	wavenumber
$S_f(\Delta\xi_0, \Delta\eta, \Delta\zeta, \omega)$	cross-power spectral density of pressure
$S_w(\Delta\xi_0, \Delta\eta, \Delta\zeta, \omega)$	cross-power spectral density of displacement
$S_p(\Delta\xi, \Delta\eta, \Delta\zeta, \omega)$	cross-power spectral density of noise inside shell

## 1. INTRODUCTION

The sound generation of a moving shell with small length to width ratio in water was studied in this paper. The shell differs from a flat plate or a slender column shell <sup>(1)</sup> in air or a buoyant body <sup>(2)</sup> with no longitudinal-pressure gradient in water. The effect of some kinds of housing on flow noise was measured by Dittman <sup>(3)</sup>. The pressure fluctuations on a plate in the region of flow separation was studied by Fricke <sup>(4)</sup>.

The present author has measured fluctuating pressures over the surface of closed shells and has analysed their correlation characteristics. By using Curle's theory on aerodynamic noise, the relation of noise field outside the shell and its resistance coefficient is obtained. The power spectral density of the noise inside the shell is estimated by taking account of the acoustic pressure coupled with the vibration of the shell.

The present paper compares the levels of power spectral density of noise inside the shell and their resistance by using two shells of different shape. Noise measurements on another shell of revolution with a projected ring was also carried out.

## 2. PRESSURE FLUCTUATION OVER THE SHELL SURFACE

The interaction between the moving shell and the surrounding fluid results in the pressure fluctuation over the shell surface. Even though the flow field is uniform, the turbulent boundary layer with pressure fluctuations is generated at the surfaces, when the Reynolds number approaches to  $10^6$ . The fluctuating pressure is greater than that in the laminar region. Because the shells discussed are blunt, the pressure gradient not only changes the speed profile of the turbulent region <sup>(5)</sup>, but also introduces the separation phenomenon <sup>(6)</sup> around the rear of the shell. Distinction of flow regimes as shown in fig. 1-1 is taken from a wind tunnel experiment. It is shown that there is obviously flow separation behind position 13 (the wind speed is 40 m/sec). The pressure fluctuation and shell vibration excited by it generate noise field outside and inside the shell.

The fluctuating pressures over different parts of the surface were measured in the towing tank. Fig. 2 shows the schematic diagram of the experiment. The measurements were performed by micro-hydrophones with preamplifiers. A tape recorder, model TEAC-SR30, was used. The results show that a laminar boundary layer with small pressure fluctuations is generated at the front part of the shell, while a turbulent boundary layer accompanied by maximum pressure fluctuation is observed at the middle of the shell. Large pressure fluctuations appear around the rear part of the shell, with frequencies lower than 5 kHz. The local Reynolds number at position 8 is about  $3 \times 10^6$ , while at position 1: about  $1.4 \times 10^5$  for an onset flow of 6.5 m/sec. Fig. 3 shows that fluctuating pressures at position 8 (in the turbulent region) are greater than at position 1 (in laminar region). Position 8 is in the region of the maximum adverse gradient. However, flow separation only occurs at position 15.

Results of signal processing show that the cross-power spectral density of pressures between two points spaced longitudinally decrease with frequency more slowly than that of two points spaced laterally. Namely, the coefficients of cross-correlation between pressures measured lengthwise are higher than those measured sectionwise.

### 3. RADIATION FIELD OF SOUND INSIDE/OUTSIDE THE SHELL

Fluctuating pressures at the surface of the shell give only small contributions to the total resistance. However, they play an important role in the generation of noise. Fluctuating pressures consist of both normal surface pressure and shear - stress<sup>(7,8)</sup>.

The total frictional resistance acting on a unit area of the shell surface consists of both the mean resistance  $T_f$  and the fluctuating resistance  $F_f$ , writing:

$$T_f = \frac{1}{2} \bar{C}_f U_0^2 = T_f + F_f \quad (1)$$

The frictional resistance coefficient  $\bar{C}_f$  is actually a function of relative fluctuating velocity  $U_f/U_0$ . Since fluctuating velocity  $U_f$  is much smaller than the onset flow  $U_0$ ,  $\bar{C}_f$  may be expressed in a power series:  $\bar{C} = C_f \{ a_0 + a_1 \frac{U_f}{U_0} + a_2 (\frac{U_f}{U_0})^2 + \dots \}$ . But the constant part of  $\bar{C}_f$  does not generate any noise, therefore the fluctuating pressure of resistance  $F_f$  is to the first order of approximation:

$$F_f \propto \rho C_f U_0 U_f \quad (2)$$

From (9), it is seen that it is impossible to produce a uniform force without also producing a fluctuating component. By similar dimensional analysis, the fluctuating form resistance can also be given to the first order of approximation by following form:

$$F_r \propto \rho C_r U_0 U_f \quad (3)$$

Starting with equations (2) and (3), the radiation fields of the sound inside and outside the shell can be discussed.

#### 3.1. Radiation field of the sound outside the shell

Since the velocity of the moving shell is much smaller than the sound velocity, the Mach number is very small.

The sound field outside the shell can be described generally at low Mach numbers using Curle's theory<sup>(10)</sup> for aerodynamic noise.

$$p(x, t) = \frac{1}{4\pi} \frac{\partial}{\partial x_i} \iint_s \frac{1}{r} (F_i)_{\bar{t}} ds - \frac{1}{4\pi} \iint_s \frac{1}{r} \left( \frac{\partial(\rho U_n)}{\partial t} \right)_{\bar{t}} ds \quad (4)$$

where square brackets ( ) denote evaluation at the retarded time  $\bar{t} = t - r/c$ .

We assume that pressure fluctuations are stationary random variables. Hence, the sound pressure and its cross-correlation in the far-field can be written in the following form:

$$\begin{aligned} p(\vec{x}, t) &= - \frac{1}{4\pi} \iint_s \frac{1}{rc} \frac{\partial r}{\partial x_i} \left( \frac{\partial F_i}{\partial t} \right)_{\bar{t}} ds - \frac{1}{4\pi} \iint_s \frac{1}{r} \left( \frac{\partial(\rho U_n)}{\partial t} \right)_{\bar{t}} ds \\ \langle p(\vec{x}, t) p(\vec{x}', t') \rangle &= \frac{1}{16\pi^2} \left\{ \iint_s \frac{1}{rc} \frac{\partial r}{\partial x_i} \left( \frac{\partial F_i}{\partial t} \right)_{\bar{t}} ds \right. \\ &\quad \left. + \iint_s \frac{1}{r} \left( \frac{\partial(\rho U_n)}{\partial t} \right)_{\bar{t}} ds \right\} \cdot \left[ \iint_{s'} \frac{1}{rc} \frac{\partial r}{\partial x_i} \left( \frac{\partial F_i'}{\partial t} \right)_{\bar{t}'} ds' + \iint_{s'} \frac{1}{r} \left( \frac{\partial(\rho U_n)}{\partial t} \right)_{\bar{t}'} ds' \right] \end{aligned} \quad (5)$$

From (2), (3),  $F_i \propto \rho U_i U_0 C_i$ . Here, it is further assumed that

$$\begin{aligned} \iint_{s'} \left\langle \frac{\partial U_i}{\partial t} \cdot \frac{\partial U_i'}{\partial t} \right\rangle ds' &= A_c \left\langle \left( \frac{\partial U_i}{\partial t} \right)^2 \right\rangle \\ \iint_{s'} \left\langle \frac{\partial U_n}{\partial t} \cdot \frac{\partial U_n'}{\partial t} \right\rangle ds' &= A_c \left\langle \left( \frac{\partial U_n}{\partial t} \right)^2 \right\rangle \end{aligned}$$



Hence, the sound intensity  $I(\vec{x}, t)$  can be expressed as:

$$I(\vec{x}, t) \propto -\frac{\rho U_0^2 C_i^2}{16\pi^2 r^2 c^3} \iint_S \left( \frac{\partial r}{\partial x_i} \right)^2 < \left( \frac{\partial U_i}{\partial t} \right)^2 > A_{cds} \\ + \frac{\rho C_i U_0}{8\pi^2 r^2 c^2} \iint_S \left( \frac{\partial r}{\partial x_i} \right) < \frac{\partial U_i}{\partial t} \cdot \frac{\partial U_n}{\partial t} > ds \\ + \frac{\rho}{16\pi^2 r^2 c} \iint_S < \left( \frac{\partial U_n}{\partial t} \right)^2 > A_{nds} \quad (6)$$

For a flat plate, if the size of the source is very small compared with  $r$ , then  $\frac{\partial r}{\partial x_i} = \cos\theta$ . For rigid walls, we have  $\frac{\partial U_n}{\partial t} = 0$ , hence,

$$I(x, t) \propto -\frac{\rho U_0^2 C_i^2 \cos^2\theta}{16\pi^2 r^2 c^2} \iint_S < \left( \frac{\partial U_i}{\partial t} \right)^2 > A_{cds} \quad (7)$$

As seen from equation (6), the sound intensity outside the shell can be divided into three parts. The first part is due to the reaction of the rigid shell to the fluctuating velocity, and is proportional to the square of the speed and square of the resistance coefficient of the shell. The second part is from interaction between the fluctuating velocity and the shell vibration and the third part is outside the shell vibration excited by the fluctuating velocity.

The fluctuating velocity  $U_i$  differs from the normal vibration velocity of the shell  $U_n$  here, and  $U_i$  can be expressed by its normal and tangential components.

### 3.2. Power spectral density of the sound inside thin shells

In general, shell vibration can be expressed in generalized coordinates  $(\xi, \eta, \zeta)$  and their eigenfunctions are  $R_n(r_{mn}\xi)$ ,  $\phi_n(\eta)$  and  $H_m(\zeta)$ .

The displacement equation of the shell neglecting tangential forces can be written as (it is assumed that the  $F(\xi_0, t)$  is uniform):

$$M\ddot{W} + R\dot{W} + DW = F(\xi_0, t) + p_1(\xi_0, t) - p_2(\xi_0, t) \quad (8)$$

The wave equations of the sound inside and outside the shell are:

$$\nabla^2 p_2 - \frac{1}{c^2} \frac{\partial^2 p_2}{\partial t^2} = 0 \\ \nabla^2 p_1 - \frac{1}{c^2} \frac{\partial^2 p_1}{\partial t^2} = 0 \quad (9)$$

with boundary conditions at the surfaces:

$$W = \frac{1}{\omega^2 \rho} \nabla p \quad (10)$$

The Fourier transformation of the displacement in frequency and time domain gives:

$$W(\xi_0, \omega) = -\frac{1}{2\pi} \int_{-\infty}^{\infty} W(\xi_0, t) e^{-i\omega t} dt \quad (11)$$

The displacement  $W$ , the sound pressure  $P_i$  and the fluctuating pressure  $F$  can be expanded by generalized coordinates:

$$W(\xi_0, \eta, \zeta, \omega) = \sum_{m,n} W_{mn}(\omega) \phi_n(\eta) H_m(\zeta) \\ \{ \quad P_i(\xi, \eta, \zeta, \omega) = \sum_{m,n} P_{imn}(\omega) R_n(r_{mn}\xi) \phi_n(\eta) H_m(\zeta) \\ F(\xi_0, \eta, \zeta, \omega) = \sum_{m,n} F_{mn}(\omega) \phi_n(\eta) H_m(\zeta) \quad (12)$$

Using equation (10) and (11), we obtain

$$W(\xi_0, \eta, \zeta, \omega) = \sum_{m,n} \frac{1}{\omega^2 \rho} \left( \frac{\partial R_n(r_{mn}\xi)}{\partial \xi} \Big|_{\xi=\xi_0} \right) P_{imn}(\omega) \phi_n(\eta) H_m(\zeta)$$

$$P_{imn}(\omega) = \frac{\omega^2 \rho W_{mn}(\omega)}{\frac{\partial R_{in}(R_{mn}\xi)}{\partial \xi} \Big|_{\xi=\xi_0}} \quad (13)$$

The displacement equation of the shell using eigenfrequencies is:

$$(M(\omega_{mn}^2 - \omega^2) + i\omega R) W_{mn}(\omega) = F_{mn}(\omega) + P_{1mn}(\omega) R_{1n}(r_{mn}\xi_0) - P_{2mn}(\omega) R_{2n}(r_{mn}\xi_0) \quad (14)$$

The receptance of the shell excited by the fluctuating pressure can be written in the following form

$$H_{mn}(\omega) = \frac{W_{mn}(\omega)}{F_{mn}(\omega)}$$

$$= \frac{1}{M(\omega_{mn}^2 - \omega^2) + i\omega R - \frac{\omega^2 \rho R_{1n}(r_{mn}\xi)}{\frac{\partial R_{1n}(r_{mn}\xi)}{\partial \xi} \Big|_{\xi=\xi_0}} + \frac{\omega^2 \rho R_{2n}(r_{mn}\xi)}{\frac{\partial R_{2n}(r_{mn}\xi)}{\partial \xi} \Big|_{\xi=\xi_0}}} \quad (15)$$

From the fluctuating pressure  $F(\xi_0, t)$  and cross-correlation function, we can find the cross-power spectral density of the pressure:

$$S_F(\Delta\xi_0, \Delta\eta, \Delta\zeta, \omega) = \frac{1}{2\pi} \int_{-\infty}^{\infty} \langle F(\xi_0, \eta, \zeta, t) F(\xi_0 + \Delta\xi_0, \eta + \Delta\eta, \zeta + \Delta\zeta, t + \Delta t) \rangle e^{-i\omega t} dt$$

$$= \sum_{m,n} \sum_{p,q} \rho^2 C_1^2 U_0^2 \phi_n \phi_p H_m H_q \cdot \frac{1}{2\pi} \int_{-\infty}^{\infty} \langle U_{mn} \cdot U_{pq} \rangle e^{-i\omega t} dt \quad (16)$$

Similarly, the cross-power spectral density of the displacement can be expressed as:

$$S_W(\Delta\xi_0, \Delta\eta, \Delta\zeta, \omega) = \sum_{m,n} \sum_{p,q} H_{mn}(\omega) H_{mn}^*(\omega) S_F(\Delta\xi_0, \Delta\eta, \Delta\zeta, \omega) \phi_n \phi_p H_m H_q \quad (17)$$

The cross-power spectral density of the noise inside the shell is:

$$S_{p2}(\Delta\xi, \Delta\eta, \Delta\zeta, \omega) = \sum_{m,n} \sum_{p,q} \frac{\omega^2 \rho}{\frac{\partial R_{2n}}{\partial \xi} \Big|_{\xi=\xi_0}} \cdot \frac{\omega^2 \rho}{\frac{\partial R_{2p}}{\partial \xi} \Big|_{\xi=\xi_0}} \cdot H_{mn}(\omega) H_{mn}^*(\omega) S_F(\Delta\xi_0, \Delta\eta, \Delta\zeta, \omega) \cdot R_{2n}(r_{mn}\xi) R_{2p}(r_{pq}\xi) \phi_n(\eta) \phi_p(\eta) H_m(\zeta) H_q(\zeta) \quad (18)$$

$$S_{p2}(\Delta\xi, \Delta\eta, \Delta\zeta, \omega) = \sum_{m,n} \sum_{p,q} \frac{\omega^2 \rho}{\frac{\partial R_{2n}}{\partial \xi} \Big|_{\xi=\xi_0}} \cdot \frac{\omega^2 \rho}{\frac{\partial R_{2p}}{\partial \xi} \Big|_{\xi=\xi_0}} \cdot H_{mn}(\omega) H_{mn}^*(\omega) R_{2n}(r_{mn}\xi) R_{2p}(r_{pq}\xi) \cdot \phi_n(\eta) \phi_p(\eta) H_m(\zeta) H_q(\zeta) \left( \sum_{m,n} \sum_{p,q} \rho^2 C_1^2 U_0^2 \right)$$

$$\phi_n \phi_p H_m H_q \cdot \frac{1}{2\pi} \int_{-\infty}^{\infty} \langle U_{mn} \cdot U_{pq} \rangle e^{-i\omega t} dt \quad (19)$$

In order to reduce cross-power spectral density of the noise inside the shell, proper shaping of the surface and small response functions of the shell seem to be very important.

#### 4. EXPERIMENTAL RESULT AND ANALYSIS

Fig. 4 shows the horizontal section shape of model I and II. The ratio of length to width is 3 for model I and 2 for model II. Fig. 1 shows that at the rear part of the model II flow separation starts for wind speed beyond 20 m/sec. The pressure distribution at the surface of model I is measured in a wind tunnel test, as depicted in fig. 5. The pressure coefficient equals to approximately 0.1 at the rear of the shell, i.e. the resistance of the shell results in form resistance.

Total resistance can be separated into frictional and form resistance.

$$F_D = \frac{1}{2} \rho U_0^2 C_D S = \frac{1}{2} \rho U_0^2 (C_{rS1} + C_{fS2}) \quad (20)$$

The frictional resistance coefficient can be calculated approximately by formula (11) for the resistance of a flat plate:

$$C_f = \frac{0.076}{(\log_{10} Re - 1.88)^2} + \frac{60}{Re} \quad (21)$$

Substituting measured values of total resistance and the Reynolds number of the shell into equation (20) and (21), we are able to calculate the form resistance, frictional resistance, and the resistance coefficient for different models. The form resistances of both model I and II are higher than their frictional resistances. Moreover, the frictional resistance increases when the ratio of length to width increases, as depicted in Fig. 6.

Both models were made of glass-reinforced plastic. The levels of noise power spectral densities inside the shell are about 5 dB higher for model I than for model II (see Fig. 8). The coefficients of frictional resistance are nearly similar for the two models but the form resistance coefficient for model II is a factor 2 higher than for model I, which explains the difference between the noise levels inside the two shells.

When a projected ring was attached to the head surface of a shell, the shape of the shell is not changed very much, but its form resistance and the noise power spectral density inside the shell are increased. The noise levels can be increased by 4 or 5 dB, as shown in Fig. 9. This experiment testifies the fact that the cross-correlation coefficient is higher in the region of flow separation.

We have studied cross-correlations between the fluctuating pressures over different parts of the shell surfaces on the one side and noise received by hydrophone inside shell at position 2\* on the other. Results illustrate that the maximum coefficient of cross-correlation between positions 15 and 2\* is 0.95 and that between positions 9 and 2\* is 0.6 in the frequency region 300-400 Hz. The same coefficient becomes 0.38 between positions 15 and 2\* and 0.2 between positions 9 and 2\* in the frequency region 3-4 kHz. All are referred to an onset flow speed of 6.5 m/sec (see Fig. 10-1, 10-2).

The above results show that the sound radiation generated by separation of flow is very important. The noise inside the shell can be decreased by proper design of the surface shape of the shell to reduce flow separation and pressure fluctuations.

#### 5. CONCLUSIONS

By analysing fluctuating pressures acting on the surfaces of closed shells



and the noise inside and outside of the shells, we have found:

1. Turbulent boundary layer and flow separations appeared at the surface of shells having small ratios of length to width and high Reynolds numbers. The frequency spectra of the fluctuating pressure are different for the front part, the middle or the rear part of the shell, especially in lower frequency region.
2. The coefficient of cross-correlation of the fluctuating pressure due to flow separation is higher than due to turbulent boundary layer. The cross-power spectral densities between two positions decrease with increasing frequency less pronounced when caused by flow separation than by turbulent boundary layers.
3. The main sources of noise of the moving shell are velocity fluctuation generated by turbulent boundary layer and flow separation. The noise intensity outside the shell results from 1) the reaction of the rigid shell to the fluctuating velocity, 2) interaction between the fluctuating pressure and the shell vibration, and 3) the vibration of the shell excited by the fluctuating velocity.
4. The cross-correlation spectral density of the noise inside the shell is proportional to the resistance coefficient. The fluctuating pressure caused by flow separation is the main cause of noise. In order to reduce interior noise, proper attention should be paid to the shape of the shell.

#### REFERENCES

1. G.M. Corcos, "Resolution of pressure in turbulence", J. Acoust. Soc. Am. Vol. 35, No. 2, 1963.
2. G.P. Haddle, E.J. Skudrzyk, "The physics of flow noise", J. Acoust. Soc. Am. Vol. 46, No. 1, 1969.
3. C.W. Dittman, J.K. Vinson, J.F. Byers, "High frequency flow noise", AD920130, 1974.
4. F.R. Fricke and D.C. Stevenson, "Pressure fluctuations in a separated flow region", J. Acoust. Soc. Am. Vol. 44, 1968.
5. H.H. Sahloemer, "Effects of pressure gradients on turbulent boundary layer wall-pressure fluctuations", J. Acoust. Soc. Am. Vol. 42, No. 1, 1967.
6. J. Katz, "Cavitation phenomena within regions of flow separation", J. Fluid Mech. Vol. 140, 1984.
7. M.S. Howe, "The role of surface shear stress fluctuations in the generation of boundary layer noise", J. Sound and Vibration, Vol. 65, No. 2, 1979.
8. A.P. Dowling, "Sound generation by turbulence near an elastic wall", J. Sound and Vibration, Vol. 90, No. 3, 1983.
9. Ross, "Mechanics of underwater noise", 1976.
10. Y.S. Pan, "Noise radiation from turbulent flow over compliant surface", AIAA paper, 1975.
11. P.S. Granville, "Elements of the drag of underwater bodies", AD/A — 03985, 1976.



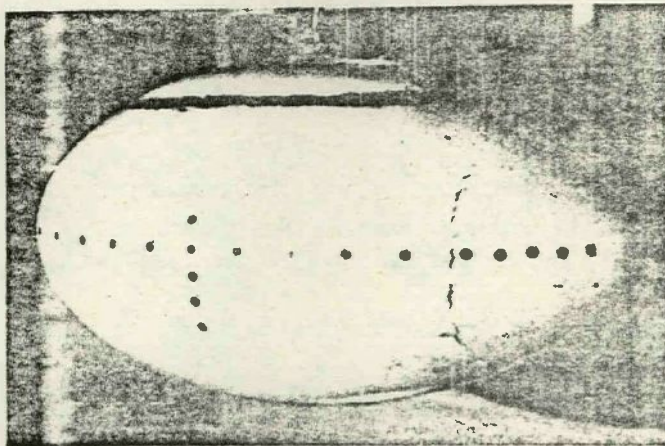


FIGURE 1-1. Distinction of flow regimes in wind tunnel.

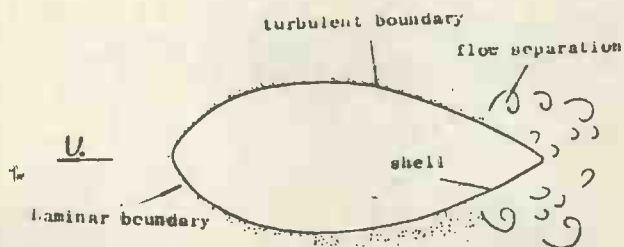


FIGURE 1-2. Schematic diagram of noise sources at a moving shell.

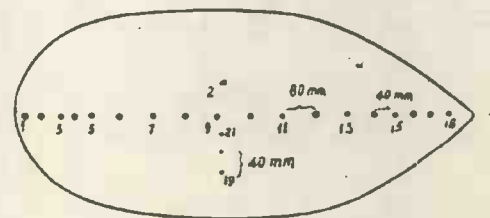


FIGURE 2. Diagram of experiment.

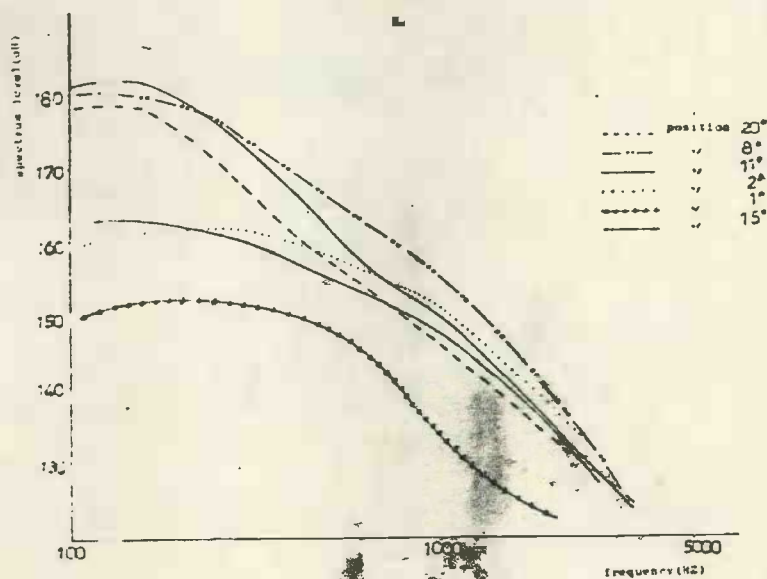


FIGURE 3. Comparison between the fluctuating pressures of the different positions at the shell surfaces at 6.5 m/sec.

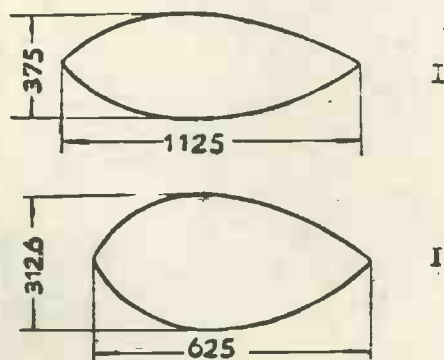


FIGURE 4. Horizontal section shape of model I and II. measures in mm.

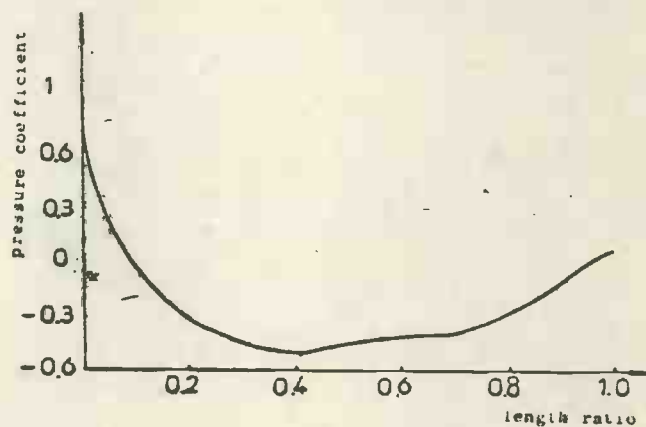


FIGURE 5. Pressure distribution on the surfaces along the longitudinal length for model I.

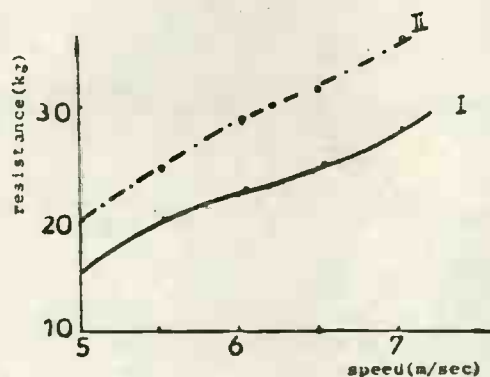


FIGURE 6. Resistance curves of model I and II.

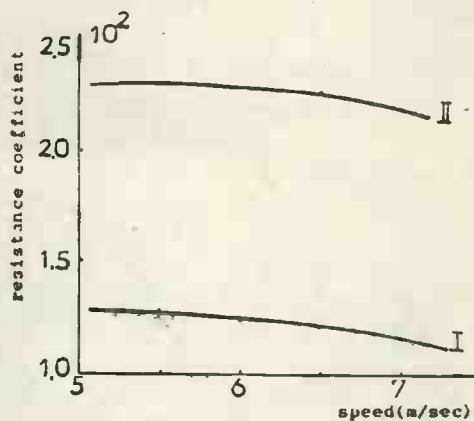


FIGURE 7. Resistance coefficients of two models versus speed.

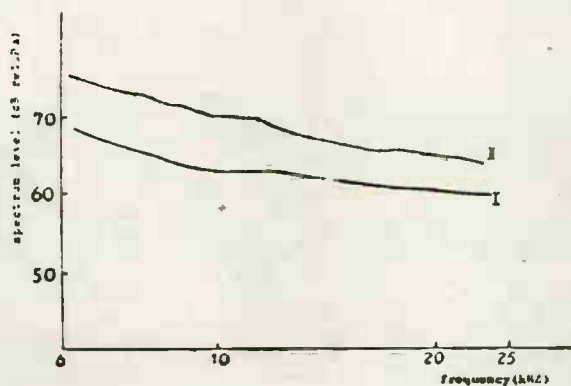


FIGURE 8. Comparison between the noise levels inside the shells of the two models at 7.5 m/sec.

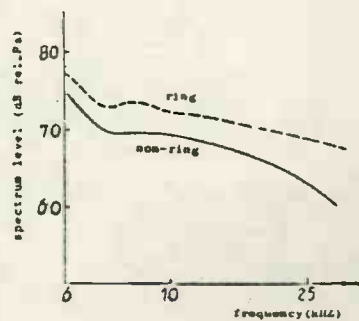


FIGURE 9. Effect of a projected ring on the sound levels inside the shell at 6 m/sec.



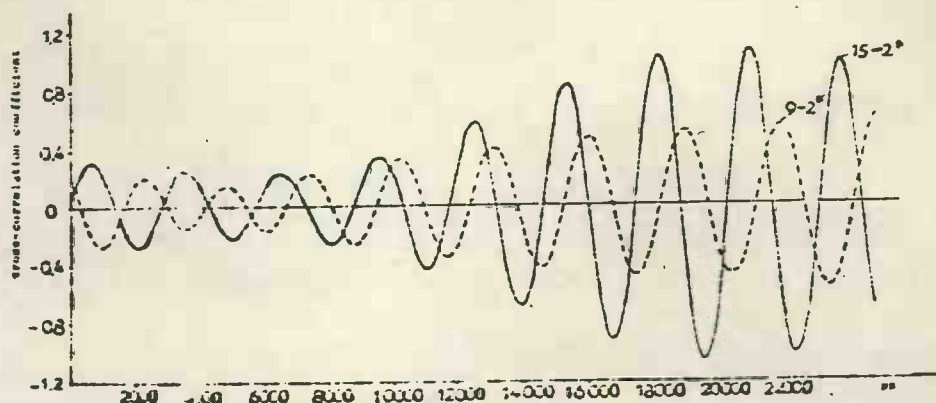


FIGURE 10-1. Cross-correlation between the fluctuating pressures at different positions at the shell surface and the noise inside the shell in the frequency region 300-400 Hz at 6.5 m/sec.

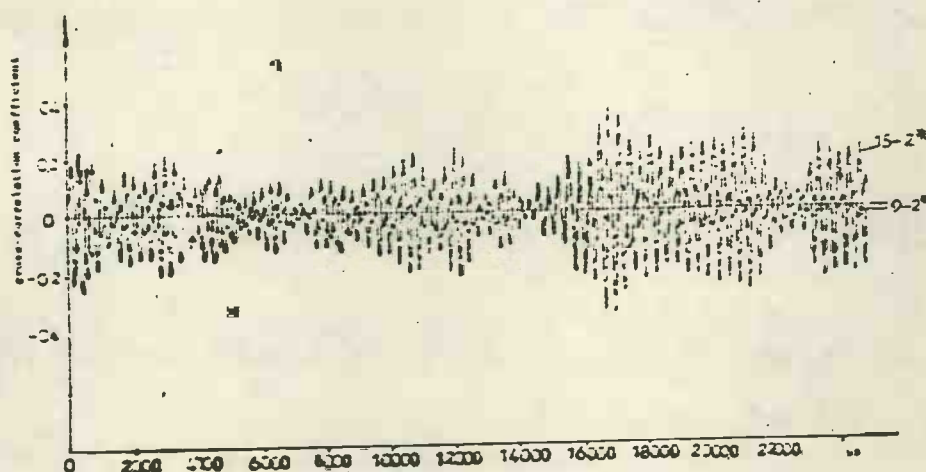


FIGURE 10-2. Cross-correlation between the fluctuating pressures at different positions at the shell surfaces and the noise inside the shell in the frequency region 3-4 kHz at 6.5 m/sec.